

Compound-Nucleus Cross Sections from Nuclear Charge-Density Distributions

D. Horn and A. J. Ferguson

Atomic Energy of Canada Limited, Chalk River Nuclear Laboratories, Chalk River, Ontario, Canada, K0J 1J0
(Received 6 July 1978)

Compound-nucleus cross sections from heavy-ion reactions are here parametrized by two terms: one for the compound nucleus and one for the entrance channel. The former is simply based on $A_{\text{cn}}^{1/3}$; the latter involves the tails of the nuclear charge-density distributions for the projectile and target. Excellent agreement is obtained with a wide range of experimental excitation functions. No parameter adjustments, even between the lightest and heaviest systems, are necessary.

Heavy-ion compound-nucleus cross sections (σ_{cn}), generally measured as the sum of fission and evaporation-residue cross sections, have been described with success in the models of Glas and Mosel¹⁻³ and of Bass.⁴⁻⁶ A shortcoming of the former model, however, is the number of free parameters (five) to be fitted for each projectile-target system. Bass offers a set of universal parameters, but to obtain good fits to a wide range of systems at energies both above and below the abrupt change of slope where a plot of σ_{cn} vs $1/E$ turns over, several parameters need to be adjusted for each case. In his calculation of the universal potential function $g(s)$, six empirical parameters are invoked.

This Letter suggests a simpler empirical formulation which gives excellent agreement with measured cross sections throughout the range of systems examined: $^{14}\text{N} + ^{12}\text{C}$ to $^{35}\text{Cl} + ^{124}\text{Sn}$. Agreement is found for energies from just above the Coulomb barrier, $1.2E_c$, to beyond the energy E_1 for which Bass⁵ predicts the onset of tangential friction. This range includes the kink at which Glas and Mosel change potential and radius parameters from their "barrier" to "critical" values. Our results are obtained using empirical charge-density distributions⁷ and making no parameter adjustments throughout the range of energies and systems studied.

From a simple classical argument as well as from a wave mechanical derivation assuming the sharp-cutoff approximation (see Scobel *et al.*⁸ for a brief discussion), the compound-nucleus cross section may be written as

$$\sigma_{\text{cn}}(E) = \pi R^2 [1 - V(R)/E], \quad (1)$$

where R is the distance of closest approach, $V(R)$ is the potential at R , and E is the incident energy in the center-of-mass system. If $V(R)$ were taken simply as the Coulomb potential, then at low energies Eq. (1) might be a reasonable approximation to the fusion cross section for fixed

fusion distance R . Clearly this would be a gross oversimplification, since with increasing incident energies the nuclear interaction should be of increasing significance. Rather than including the nuclear potential in V , we introduce a varying parameter, ρ , in place of the fixed distance R . If we define the collision distance, $D = Z_1 Z_2 e^2 / E$ as the product of target and projectile nuclear

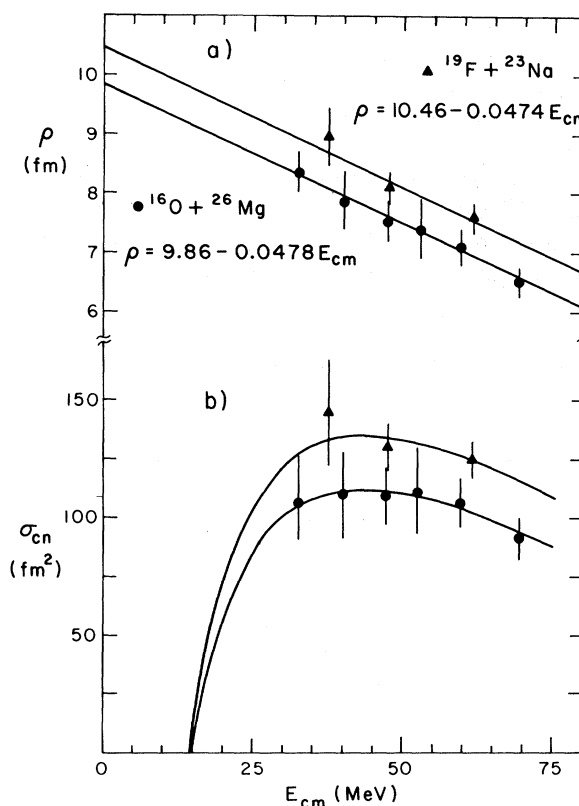


FIG. 1. (a) Comparison of the parameter ρ for ^{42}Ca formed by $^{19}\text{F} + ^{23}\text{Na}$ and by $^{16}\text{O} + ^{26}\text{Mg}$, showing linearity in E_{cm} . Similar slopes but different intercepts are obtained. (b) Experimental fusion cross sections from which ρ was obtained using $\sigma_{\text{cn}} = \pi\rho(\rho - D)$. The data are from Ref. 9.

TABLE I. Parameters for calculation of $\rho = mE + b$. b is the sum of radii at 1.35% of central density for target and projectile. Charge-density distributions are taken from Ref. 7 and the value for ^{35}Cl is estimated from systematics of radii. m is calculated from Eq. (4).

System	b (fm)	m (fm/MeV)
$^{14}\text{N} + ^{12}\text{C}$	8.71	-0.0758
$^{19}\text{F} + ^{12}\text{C}$	9.25	-0.0610
$^{32}\text{S} + ^{24}\text{Mg}$	10.83	-0.0348
$^{32}\text{S} + ^{27}\text{Al}$	10.83	-0.0334
$^{35}\text{Cl} + ^{27}\text{Al}$	11.12	-0.0322
$^{35}\text{Cl} + ^{48}\text{Ti}$	12.02	-0.0261
$^{35}\text{Cl} + ^{62}\text{Ni}$	12.43	-0.0235
$^{35}\text{Cl} + ^{116}\text{Sn}$	13.56	-0.0179
$^{35}\text{Cl} + ^{124}\text{Sn}$	13.57	-0.0174

charges divided by energy, then

$$\sigma_{\text{cn}}(E) = \pi\rho(\rho - D). \quad (2)$$

This is not to say that we expect the true potential to be Coulomb in nature, but that within Eq. (2), ρ is required to compensate for effects of the nuclear interaction.

We have investigated how ρ must vary so that the observed experimental fusion cross sections⁸⁻¹³ can be represented by Eq. (2). Over the range of energies specified ($1.2E_c$ to $E1$), a simple linear relationship is observed, i.e.,

$$\rho = mE + b, \quad (3)$$

where $m = d\rho/dE$ is the slope and b is the inter-

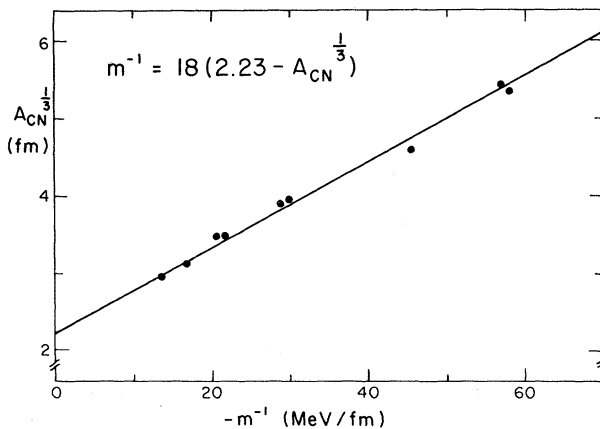


FIG. 2. $A_{\text{cn}}^{1/3}$ of the compound nucleus plotted as a function of $-1/m$ for compound nuclei from ^{26}Al to ^{159}Ho . m was obtained from Refs. 8-13 after b was fixed as the distance between centers for overlap to 1.35% of the central density.

cept in plots of the type shown in Fig. 1(a). This figure, and the cross-section plot [Fig. 1(b)] show data for the same compound nucleus, ^{42}Ca , made by two different reactions.⁹ The fact that the two lines in Fig. 1(a) have the same slope but different intercepts suggests that m may be dependent on the compound nucleus and b on the entrance channel. Starting with this possibility, we investigate the systematics of the two quantities with a view toward establishing general expressions for them.

Two-parameter (m and b) fits to the data give $b \cong 1.80(A_1^{1/3} + A_2^{1/3})$ with deviations of up to 8% in the coefficient for various systems. A more uni-

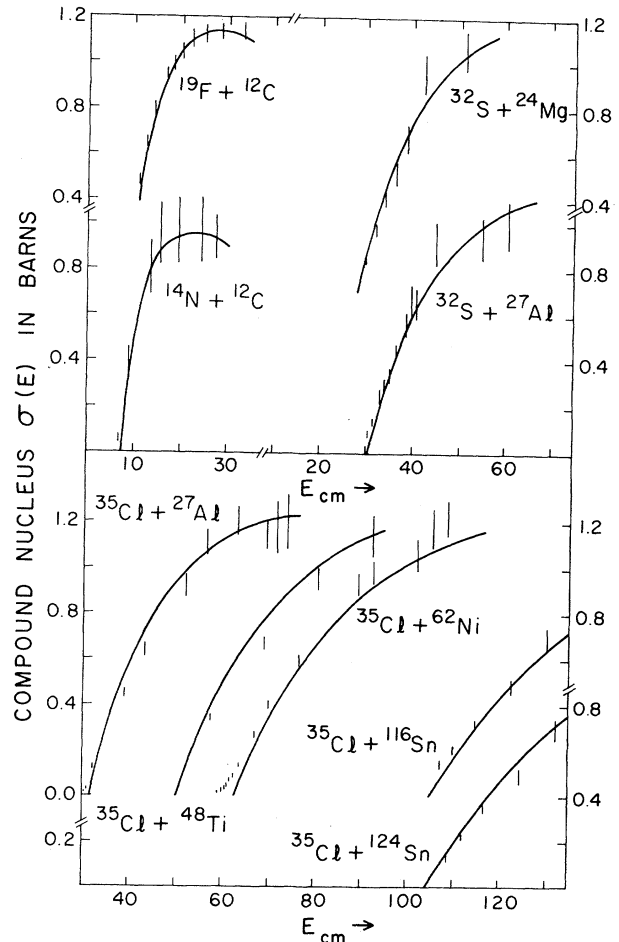


FIG. 3. Compound-nucleus excitation functions calculated from nuclear charge-density distributions using Eqs. (4) and (5). The values of m and b obtained are listed in Table I. No parameters are adjusted between the lightest and heaviest systems. The vertical bars are experimental points: $^{14}\text{N} + ^{12}\text{C}$ from Ref. 10, $^{19}\text{F} + ^{12}\text{C}$ from Refs. 11 and 12, ^{32}S reactions from Ref. 13, and ^{35}Cl reactions from Ref. 8.

form expression for b may be obtained from an examination of experimental nuclear charge-density distributions.⁷ Defining "contact" as overlap to 1.35% of the central density for each of both target and projectile universally reproduces b as the distance between centers. A choice of, e.g., 1.20% would give b 's larger by ~ 0.15 fm. Values obtained are listed in Table I. b would then seem to be the distance at which the nuclear potential becomes significant. In this connection, one might conjecture that the nuclear matter-density distribution should be of greater significance than the more readily available charge distribution.

With b established, $m = n^{-1} \sum_i (\rho_i - b)/E_i$ is easy to extract from experimental excitation functions with n energy points. A plot of m^{-1} (MeV/fm) versus a simple compound-nucleus radius, taken as $A_{\text{cn}}^{1/3}$ (fm) (see Fig. 2) reveals a convincing linearity:

$$m^{-1} = 18(2.23 - A_{\text{cn}}^{1/3}). \quad (4)$$

Values of m calculated from (4) are listed in Table I. Both the dimensionality and the magnitude of the coefficient on the right-hand side of Eq. (4) correspond to the liquid-drop surface-energy parameter, $a_s = 18$ MeV/fm². The quantity m^{-1} has the dimensions of a potential gradient and mE is the amount by which the nuclear potential reduces b to yield ρ at a given incident energy. The reader should be cautioned that though it is perhaps an analogous quantity, m^{-1} is not the actual potential gradient of the system at $\rho(E)$.

Simply fitting m and b to individual excitation functions (Fig. 1), one obtains excellent agreement with data by using these two parameters where previous models required more. What is of greater interest, however, is that it is now possible to calculate $\sigma_{\text{cn}}(E)$ for the entire range of heavy-ion systems^{8,10-13} using only the experimental radii at 1.35% charge density⁷ and m as expressed in Eq. (4). This has been done for representative systems from $^{14}\text{N} + ^{12}\text{C}$ to $^{35}\text{Cl} + ^{124}\text{Sn}$ and the results are shown in Fig. 3 (see also Table I). Note that there are no adjustments in the calculation between the lightest and the heaviest systems. The systems of Fig. 1, $^{19}\text{F} + ^{23}\text{Na}$ and $^{16}\text{O} + ^{26}\text{Mg}$ are discussed in greater detail in Ref. 9.

In a recent presentation of fusion systematics Kovar *et al.*¹⁴ point out that, in contrast to predictions, the maximum observed fusion cross section for $^{15}\text{N} + ^{12}\text{C}$ substantially exceeds that of other p -shell projectiles on carbon. For exam-

ple, the experimental maximum for ^{15}N is greater than that for ^{14}N by 19%. Despite the fact that we use charge distributions rather than matter distributions, our calculations obtain a 12% increase in cross section for ^{15}N over ^{14}N . This is encouraging and may be attributed to the fact that though the rms charge radius only varies by 0.04 fm⁷ between the two isotopes, the radius at 1.35% (of central density) changes by 0.23 fm. Expressed as a percentage of the radius, the change is more than three times as great at the tail of the potential as at the rms radius, and further underscores the importance of the tail of the nuclear potential in compound-nucleus reactions.

A survey of greater scope, fitting m and b to experimental cross sections in the equation

$$\sigma_{\text{cn}}(E) = \pi(m^2 E^2 + 2mEb + b^2 - mZ_1Z_2e^2 - bZ_1Z_2e^2/E) \quad (5)$$

may yield improved values for the constants in Eq. (4) and for the density determining b , particularly if a good measurement of the charge-density distribution of ^{35}Cl were available.

Helpful discussions with Dr. O. Häusser are gratefully acknowledged. One of us (D.H.) acknowledges receipt of a National Research Council of Canada Postdoctoral Fellowship.

¹D. Glas and U. Mosel, Phys. Lett. **49B**, 301 (1974).

²D. Glas and U. Mosel, Phys. Rev. C **10**, 2620 (1974).

³D. Glas and U. Mosel, Nucl. Phys. **A237**, 429 (1975).

⁴R. Bass, Phys. Lett. **47B**, 139 (1973).

⁵R. Bass, Nucl. Phys. **A231**, 45 (1974).

⁶R. Bass, Phys. Rev. Lett. **39**, 265 (1977).

⁷C. W. de Jager, H. de Vries, and C. de Vries, At. Data Nucl. Data Tables **14**, 479 (1974).

⁸W. Scobel, H. H. Gutbrod, M. Blann, and A. Mignerey, Phys. Rev. C **14**, 1808 (1976).

⁹D. Horn, A. J. Ferguson, and O. Häusser, to be published.

¹⁰R. G. Stokstad, R. A. Dayras, J. Gomez del Campo, P. H. Stelson, C. Olmer, and M. S. Zisman, Phys. Lett. **70B**, 289 (1977).

¹¹B. Kohlmeyer, W. Pfeffer, and F. Pühlhofer, Nucl. Phys. **A292**, 288 (1977).

¹²P. Sperr, T. H. Braid, Y. Eisen, D. G. Kovar, F. W. Prosser, J. P. Schiffer, and S. L. Tabor, Phys. Rev. Lett. **37**, 321 (1976).

¹³H. H. Gutbrod, W. G. Winn, and M. Blann, Nucl. Phys. **A213**, 267 (1973).

¹⁴D. G. Kovar, K. Daneshevar, D. F. Geesaman, W. Henning, F. W. Prosser, K. E. Rehm, J. P. Schiffer, and S. L. Tabor, in *Proceedings of the International*

Conference on Nuclear Structure, Tokyo, Japan, 1977, edited by The Organizing Committee (International Academic Printing Co. Ltd., Tokyo, 1977).

New Isovector Collective Modes in Deformed Nuclei

N. Lo Iudice

Istituto di Fisica Teorica dell'Università di Napoli, Napoli, Italy, and Istituto Nazionale di Fisica Nucleare, Sezione di Napoli, Napoli, Italy

and

F. Palumbo

Istituto Nazionale di Fisica Nucleare, Laboratori Nazionali di Frascati, Frascati, Italy
(Received 13 February 1978)

We study a model of a deformed nucleus in which protons and neutrons are described as interacting rigid rotors with axial symmetry. The nucleus as a whole is no longer axially symmetric. A magnetic-dipole collective state describing rotational oscillations of protons against neutrons is predicted.

The electric dipole giant resonance is an isovector collective excitation existing in all nuclei. It has a semiclassical interpretation as a translational oscillation of protons against neutrons.¹ This two-fluid picture suggests the existence of additional modes of excitation in deformed nuclei. For instance, the neutron and proton deformed fluids might perform rotational oscillations of opposite phase around a common axis,² generating an isovector magnetic resonance.²

In this paper we study the properties of a deformed nucleus in which protons and neutrons are described as identical rigid rotors with axial symmetry. The orientation of the two rotors is completely specified by the Euler angles α_p , β_p , α_n , and β_n needed to identify their symmetry axes $\hat{\xi}_p$ and $\hat{\xi}_n$.

If relative translational motion is excluded, the kinetic energy of the whole system about its center of mass is

$$T = (1/2\mathcal{G}_0)[(I_{\xi_p}^{(p)})^2 + (I_{\eta_p}^{(p)})^2 + (I_{\xi_n}^{(n)})^2 + (I_{\eta_n}^{(n)})^2], \quad (1)$$

where $I_{\xi_p}^{(p)}$, $I_{\eta_p}^{(p)}$, $I_{\xi_n}^{(n)}$, and $I_{\eta_n}^{(n)}$ are the components of the angular momenta of protons and neutrons along their respective principal axes $\hat{\xi}_p$, $\hat{\eta}_p$, $\hat{\xi}_n$, and $\hat{\eta}_n$ (which are arbitrary) and \mathcal{G}_0 is their common moment of inertia. Rotations around the symmetry axes are excluded.

We assume the potential to be a function of the angle between the symmetry axes $\hat{\xi}_p$ and $\hat{\xi}_n$, which we denote by 2θ . It is then convenient to express T in a form which exhibits its θ dependence. To this end we define the principal axes for the

whole nucleus:

$$\begin{aligned} \hat{\xi} &= \frac{1}{\sin(2\theta)} \hat{\xi}_p \times \hat{\xi}_n, \\ \hat{\eta} &= \frac{1}{2\sin\theta} (\hat{\xi}_p - \hat{\xi}_n), \\ \hat{\xi} &= \frac{1}{2\cos\theta} (\hat{\xi}_p + \hat{\xi}_n), \end{aligned} \quad (2)$$

and the O(4) generators $\hat{\mathbf{I}} = \hat{\mathbf{I}}^{(p)} + \hat{\mathbf{I}}^{(n)}$ and $\hat{\mathbf{S}} = \hat{\mathbf{I}}^{(p)} - \hat{\mathbf{I}}^{(n)}$. As will be shown in a more detailed presentation of this work, the commutation relations of the components of $\hat{\mathbf{I}}$ and $\hat{\mathbf{S}}$ are satisfied if we put

$$S_\xi = i\frac{\partial}{\partial\theta}, \quad S_\eta = -\cot\theta I_\xi, \quad S_\zeta = -\tan\theta I_\eta. \quad (3)$$

We can now replace the four dynamical variables α_p , β_p , α_n , and β_n by the Euler angles identifying the principal axes and θ . The correspondence is one to one if we allow the Euler angles to vary over their full range and θ to vary between zero and $\frac{1}{2}\pi$. In order to express the Hamiltonian in the new variables we observe that the kinetic energy can also be written

$$T = \frac{1}{2\mathcal{G}_0} [(I^{(p)})^2 + (I^{(n)})^2] = \frac{1}{4\mathcal{G}_0} (I^2 + S^2) \quad (4)$$

with the constraint

$$I_{\xi_p}^{(p)} = I_{\xi_n}^{(n)} = 0.$$

These constraints are automatically satisfied by the realization (3) of $\hat{\mathbf{S}}$. We can therefore